

## ENHANCED POWER CONVERSION EFFICIENCY OF DYE SYNTHESIZED SOLAR CELL BY FEW LAYERED GRAPHENE/CuO NANOCOMPOSITE AS A WORKING ELECTRODE

B. SATISH<sup>a</sup>, V. RAJENDAR<sup>b\*</sup>, K. V. RAO<sup>a</sup>, C. S. CHAKRA<sup>a</sup>

<sup>a</sup>*Nanoelectronics Lab, Center for Nanoscience and Technology, IST, Jawaharlal Nehru Technological University Hyderabad, Telangana State, 500085, India.*

<sup>b</sup>*Department of Electronic Engineering, Yeungnam University, Gyeongsan-si Gyeongsangbuk-do 38541, Republic of Korea*

In this current research, we described an enhanced power conversion efficiency of dye sensitized solar cell (DSSC) and fabricated through Few Layered Graphene (FLG)/CuO nanocomposite synthesized by ultrasonic assisted synthesis (UAS) by varying of FLG (1, 2 and 3 wt%) ratio. The FLG/CuO nanocomposites characteristic features understood through various microscopic techniques such as FE-SEM and HR-TEM. Phase and compositional analysis carried out by XRD, band gap calculations done by UV-Vis diffuse reflectance spectra (UV-DRS). The prepared FLG/CuO nanocomposites were used as working electrode materials and will be deposited like thin films on already fabricated fluorine-doped tin oxide (FTO) conductive glass substrate by doctor blade technique. Studied the effect of power conversion efficiency (PCE) in DSSC application with respect to different wt% of FLG in FLG/CuO nanocomposites. The photovoltaic characteristics and current density versus voltage (J-V) analysis done with N719 dye at AM 1.5G and 100 m W/m<sup>2</sup> of the solar simulator. The PCE 2.61% is the highest for FLG (1 wt%)/CuO nanocomposite compared to CuO NPs and other working electrodes.

(Received November 21, 2016; Accepted January 20, 2017)

*Keywords:* Few-Layered Graphene; FLG/CuO nanocomposite; Working electrode; Dye-sensitized solar cell; Power conversion efficiency

### 1. Introduction

Solar cell technology is one of the future energy resources has been progressing recently. Silicon is utilized as the semiconductor material for traditional sun powered cells, yet silicon is costly and the cost diminishment of the sun oriented cells is a standout amongst the most essential issues, due to this reason introduced dye-sensitized solar cells (DSSC)[1]. The color sharpened sun powered cells (DSSC) are the third era of sun oriented cell, with the promising high change effectiveness, straightforward assembling, minimal effort, furthermore ready to use the indoor light asset. It was initially reported with the productivity of 7.1%–7.9% in 1991 [2]. General methods of planning DSSC have been investigated and created to enhance the control gathering to a sensibly elite. The present world record is more than 14% [3], accomplished by Hanaya's group in 2015. The most astounding effectiveness of DSSC with iodine electrolyte is 11.4% [4]. These solar cells utilize three main components: (1) Dye molecules will absorb the light. (2) The photo anode consists of the semiconductor material, i.e. TiO<sub>2</sub>, ZnO and WO<sub>3</sub>, with dye molecules attached to the side. (3) To regenerate electrons for the dye molecules, the conductive counter electrode will catalyze the electrolyte redox reaction [5]. As of late, graphene based materials have pulled in much consideration for promising option working terminal materials in DSSC. This work expects to enhance the transformation effectiveness of DSSC by presenting another material, graphene, into the DSSC structure[6]. Graphene is a potential material for some applications because of their high electron versatility, exceptional optical properties and warm, concoction, and

---

\* Corresponding author: rajendar.nano@gmail.com

mechanical steadiness. Subsequently, this study changes a few parameters, structures and strategies to improve and contrast the conventional DSSC. It implies that the new material, graphene, works in upgrading the change effectiveness of DSSC.

The metal oxides are dispersed on the surface of graphene or between the graphene layers, additionally viably lessen the level of the restacking of graphene and uncover more dynamic surface territory to the electrolytes [7-8]. The elements of copper oxide (CuO) semiconductors are generally higher optical ingestion, minimal effort of crude materials and non-lethal. CuO p-sort semiconductors with band crevice energies of 1.5 eV, which are near the perfect vitality hole of 1.4 eV for sun based cells and considers great sun based phantom assimilation. In this work, we presenta simple USA method tosynthesizethe FLG/CuO composites and evaluate their PCE in DSSC application. Amid the ultrasonic procedures, graphene can be totally scattered and serve as the electric conductive and CuONPsuniformly decked on the surface of FLG sheet. Thus, as expected, the FLG/CuO nanocomposite working electrodes exhibit a high PCE in DSSC.

## 2. Experimental

### 2.1. Synthesis of FLG/CuO nanocomposite

The GO was readied utilizing altered hummer's technique as a part of the nearness of the ultrasonic procedure [9]. The FLG/CuO nanocomposites combined by a Ultrasonic Qsonicasonicator (Model no: Q500, 20 KHz Frequency, 500 W) at 45% plentifulness. In this procedure, 0.5g of GO was scattered in 200ml ethanol to get a dim chestnut shading arrangement by mixing for 30 min, then 2ml of hydrazine monohydrate arrangement was included for diminishment. A suitable of cupper acetate solution get dried out was included into the above came about arrangement and after that moved into 500 ml vessel and put in a ultrasonic chamber for 2 hours sonication. At long last, the arrangement was separated and washed 3 times with refined water and dried in hot air over at 90°C for 5 hours to vanish the solvents. The consequent powder was calcination at 600°C for 4 hours in a stiffler heater. The acquired FLG/CuO nanocomposite with various weight rates (FLG 1, 2 and 3 wt%) by changing the measure of the GO. For examination, immaculate CuO NPs was likewise combined by the comparative above strategy without GO.

### 2.2. DSSC device fabrication

The working terminals cells produced using CuO and FLG (1, 2 and 3 wt%)/CuO nanocomposites powders by an indistinct procedure from reported [10]. Quickly, A thicker paste was set up by 2.0 g of CuO nanopowder was scattered in 20 ml of ethanol was using ultra sonication shower for 30 min after filled in porcelain chamber motor and pestle. Furtherly, 1ml PEG (MW 10000) added to keep up the consistency of the paste. Finally, a few drops of Triton X-100 were added to beat the surface weight property of the paste and avoid the advancement of surface breaks. At that point the glue was covered onto a FTO conductive glass substrate by specialist cutting edge method in the measurement of 1 cm x 1 cm. This substrate was reinforced at 450°C for 30min, then cooled to 35°C and submerged into the N719 (Di-tetra butyl ammonium cis-bis(isothiocyanate) bis(2,2'bipyridyl 4,4' dicarboxylato) ruthenium (II)) shading game plan with centralization of  $0.5 \times 10^{-3}$  M in ethanol for 24 hours. After shading maintenance, the film was washed with ethanol and refined water and after that used as working cathode for DSSC. Platinum (Pt) sputtered FTO substrate was used as the counter cathode. The two anodes (working and counter) were accumulated as a sandwich sort cell using two snaps. The dynamic cell scope of the amassed cell was  $0.25 \text{ cm}^2$ . Finally, the liquid electrolyte (common dissolvable based) was set up from 0.6M dimetyl propylimidazolium iodide, 0.1M of iodine, 0.5M tert-butylpyridine and 0.1M of lithium iodide in 3-methoxyacetonitrile. The space between the two cathodes stacked with few drops of the electrolyte with the help of scaled down scale pipette. The contact of the anodes was made using a silver paste. Beforehand specified procedure was taken after to make the cells for FLG (1, 2 and 3wt %)/CuO nanocomposites.

### 2.3 Characterization

The crystal phase and composition of arranged FLG/CuO nanocomposite explored by (XRD, Model no: Bruker D8 progressed) with  $\text{CuK}\alpha$  radiation ( $k=1.540\text{\AA}$ ). The retention range was recorded utilizing Ultraviolet-Visible diffuse reflectance spectrophotometer (UV-DRS, Model No: JASCO V-670). The surface morphology dissected by field emission scanning electron microscopy (FE-SEM, Model no: Carl Zeiss Merlin Compact 6027) and high determination transmission electron microscopy (HR-TEM, Model no: JEOLJEM 200CX). The current density versus voltage (J-V) parameters of the DSSC were measured by under the enlightenment of a reproduced AM1.5G sun powered light from the 450-W Xenon light (Model no: Oriel Class 3A) utilizing a sun based test system with Keithley 2440 source meter.

## 3. Results and discussion

### 3.1. Structural Analysis

The prepared CuO nanoparticles (NPs) and their nanocomposites FLG (1, 2 and 3 wt %)/CuO were confirmed by XRD. Fig. 1 demonstrates the XRD samples of the got unadulterated CuO NPs and FLG (1,2 3 wt%)/CuO individually. The characteristic diffraction planes of CuO NPs (110), ( $\bar{1}11$ ), (111), (202), (020), (202), ( $\bar{1}13$ ), (022), (022) ( $\bar{3}11$ ) (220) (311) and (004) were watched comparing their  $2\theta$  values. The outcomes are coordinated with the JCPDS File No; (05-0661) for monoclinic stage [11]. Then again, in FLG (1, 2 and 3 wt%)/CuO nanocomposites a little pinnacle is seen at ( $2\theta = 25.3^\circ$ ) which speaks to a mark of carbon (002) plane of FLG [12]. The weight percentage of FLG increment (from 1 to 3 wt%)/CuO nanocomposites the pinnacle power nearly diminish contrasted with CuO NPs. The normal crystallite measure ascertained utilizing sherr's equation [13] is found to be 22, 20, 18 and 13 nm for CuO NPs and FLG (1, 2 and 3 wt%)/CuO nanocomposite separately.

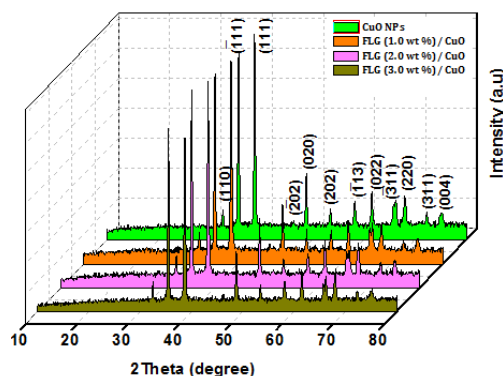


Fig 1. XRD pattern of CuO NPs and FLG (1, 2 and 3wt %)/CuO nanocomposites.

### 3.2. Optical band gap studies:

Fig. 2 shows the UV-Vis diffuse reflectance of CuO NPs and FLG (1, 2 and 3 wt %)/CuO nanocomposites. The ingestion pinnacle of CuO NPs is displayed at  $\sim 686$  nm. As prepared FLG (1, 2 and 3wt%)/CuO nanocomposites absorption peaks ( $\sim 689$ ,  $\sim 692$  and  $\sim 697$  nm) were slightly shifted compared to CuO NPs. The absorption intensity of FLG/CuO nanocomposites increases with the increases of the FLG amount, it can be shown to the increases in surface electrical charge of CuO NPs within the composite due to the introduction of the FLG. The optical band gap of as prepared CuO NPs and FLG(1, 2 and 3 wt%)/CuO nanocomposites was calculated from the absorption spectra using Tauc condition [14]. The calculated band values for CuO NPs and FLG (1, 2 and 3 wt%)/CuO nanocomposites are found to be 1.80, 1.79, 1.78, 1.77 eV independently.

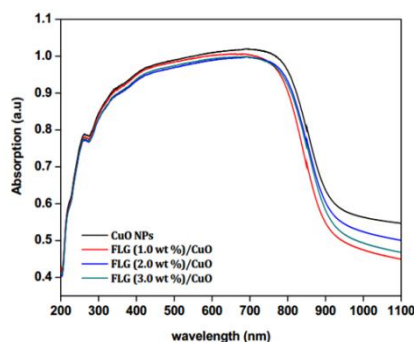


Fig 2. Optical absorption of CuO NPs and FLG (1, 2 and 3wt%)/CuO nanocomposites.

### 3.3. Morphological studies:

The morphologies of CuO and FLG(1, 2 and 3 wt%)/CuO nanocomposites were shown in Fig 3. In the images, a trend is very conspicuous and can be noted for understanding the morphological changes that are happening in these materials. The electron micrograph reveals that pure CuO NPs look like in the form of spheres shown in Fig. 3(a). And in FLG/CuO for FLG 1 wt% in Fig 3(b) looks like some of the CuO nanoparticles are decorated on FLG sheet. And further going 2 wt%, 3 wt% FLG in FLG/CuO nanocomposite, we can find that more number of CuO nanoparticles were grown on the surface due to the reaction oxygen groups (Fig 3(c-d)). And which confirms most of the CuO nanoparticles are attached to FLG sheet mostly at the edges because of the functional groups at the edges. This particular phenomenon needs to be proven by understanding the morphological properties much more closely and needs to be confirmed by analyzing the material using higher grade morphological and chemical analysis techniques.

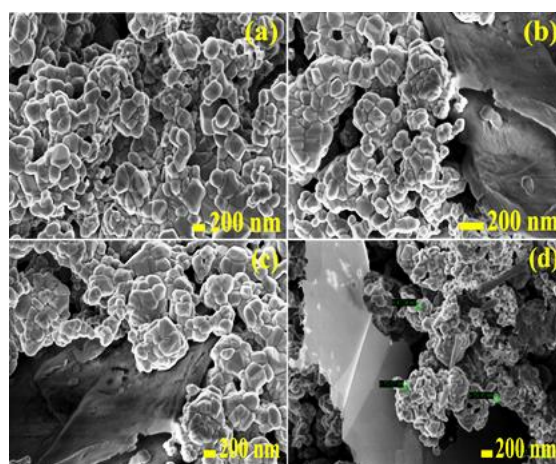


Fig 3. FE-SEM image of (a) CuO NPs, (b) FLG (1 wt%)/CuO, (c) FLG (2wt%)/CuO, (d) FLG (3 wt%)/CuO nanocomposites.

TEM results reconfirm the postulate made in the SEM analysis. The further morphologies studies were investigated by HRTEM analysis. The CuO particles are having the morphology of irregular shapes as shown in Fig. 4 (a). The CuO particles are completely decked on the FLG sheet (Fig. 4 (b-c)). Some locations CuO particles are agglomerated on the FLG sheet.

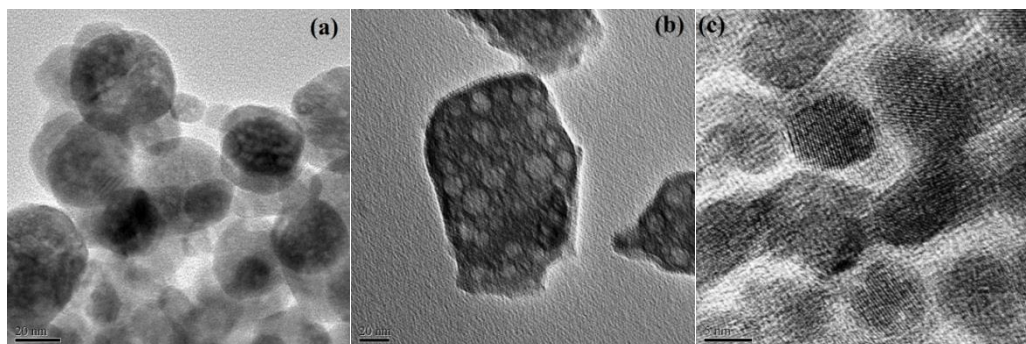


Fig 4. TEM image of (a) CuO NPs (b) FLG (1 wt%)/CuO nanocomposite (c) HRTEM image of FLG (1 wt%)/CuO nanocomposite

### 3.4 Current density - Voltage (J-V) analysis

Fig. 5 shows the photo current density versus voltage (J-V) curves of CuONPs and FLG (1, 2 and 3wt%)/CuO nanocomposites as working electrodes, under simulated 100 m W/m<sup>2</sup> illumination. The photovoltaic parameters are show in Table.1. DSSC that was fabricated with CuO working electrode showed a  $V_{oc}$  of 0.72 V, a  $J_{sc}$  of 3.64 mA/cm<sup>2</sup>, FF of 67.1% and PCE of 1.77%. On the other hand FLG (1wt %)/CuO nanocomposites as working electrodes, showed a  $V_{oc}$  of 0.73 V, a  $J_{sc}$  of 4.63 mA/cm<sup>2</sup>, FF of 78.3% and PCE of 2.68%, FLG (2wt%)/CuO,  $V_{oc}$  of 0.72 V, a  $J_{sc}$  of 3.46 mA/cm<sup>2</sup>, FF of 65.4% and PCE of 1.64% and FLG (3 wt%)/CuO,  $V_{oc}$  of 0.72 V, a  $J_{sc}$  of 2.05 mA/cm<sup>2</sup>, FF of 72.4% and PCE of 1.02%. This unique outcome, confirms that suitable proportion of (1 wt%) FLG in CuO acts as a blocking layer to smother the back electron-hole recombination in DSSC and thus enhances the power conversion efficiency.

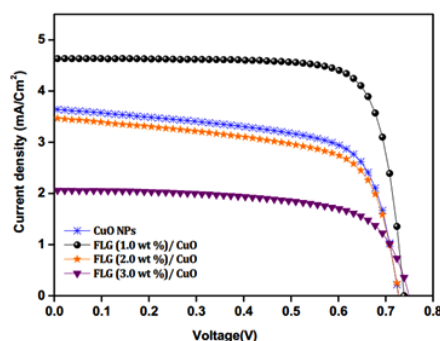


Fig 5. J-V curves of CuO and FLG (1, 2 and 3 wt%)/CuO working electrodes based DSSC.

Table 1. Photovoltaic parameters of the CuO and FLG (1, 2 and 3 wt%)/CuO working electrodes based DSSC.

Working electrodes	$V_{oc}$ (V)	$J_{sc}$ (mA/cm <sup>2</sup> )	FF (%)	PCE (%)
CuONPs	0.72	3.64	67.1	1.77
FLG (1 wt%) / CuO	0.73	4.63	78.3	2.68
FLG (2 wt%) / CuO	0.72	3.46	65.4	1.64
FLG (3wt%) / CuO	0.72	2.05	72.4	1.02

## 4. Conclusions

Successfully synthesized FLG/CuO nanocomposites by Ultrasonic assisted synthesis (UAS) method. The XRD pattern confirmed the formation of FLG/CuO nanocomposites with high

crystallinity. The characteristic absorbance peaks of FLG/CuO nanocomposites were observed in UV visible spectra. FE-SEM image revealed that the sheet like FLG decked with CuO in homogeneously. Decoration of flower shape CuO nanoparticles on FLG sheet was confirmed by HR-TEM.

The fabrication of CuONPs and FLG (1, 2 and 3 wt%)/CuO nanocomposites successfully used as working electrodes in DSSC application. A significant enhancement of (2.68%) in the power conversion efficiency was achieved in DSSC using FLG (1wt%)/CuO nanocomposite as photoanode to compare CuO NPs and to other nanocomposites FLG (2, 3 wt%)/CuO working electrodes under A.M 1.5G solar simulated. The enhancement is related to the increase of electron transfer rate in the FLG(1 wt%)/CuO nanocomposite working electrode which is originated from the high electron mobility of FLG thus enhances the power conversion efficiency. However, higher FLG loading beyond the optimal concentration has lead to the decrease of the efficiency due to the light preserving of the FLG.

## References

- [1] M. Jacoby, The future of low-cost solar cells, **94**(18), 30(2016).
- [2] N.Rawal, A.G. Vaishaly, H. Sharma, B.B. Mathew, Energy and Power Engineering Science,**2**(2),46 (2015).
- [3] B. Oregan, M. Gratzel, Nature,**353**,737 (1991).
- [4] T.H. Tsai, S.C.Chiou, S.M. Chen, K.C. Lin, Int. J. Electrochem. Sci, **6**(9), 3938 (2011).
- [5] S.Yun , A.Hagfeldt, T. Ma, Adv. Mater, **2**,66210 (2014).
- [6] S. Casaluci, M.Gemmi, V. Pellegrini, A.D.Carloa, F. Bonaccorso, Nanoscale (8), 5368(2016)
- [7] C. Peng, B. Chen, Y. Qin, S. Yang, C. Li, Y. Zuo, S. Liu, J. Yang, ACS Nano, **6**(2),1074 (2012).
- [8] G. Williams, P.V. Kamat, Langmuir, **25**(24),13869 (2009).
- [9] B. Satish, K.V. Rao, R. Nareshkumar, Ch. Shilpa Chakra, T. Dayakar, J Mater Sci: Mater Electron-2016, DOI 10.1007/s10854-016-5388-2.
- [10] B. Satish, K.V. Rao, Ch. Shilpa Chakra, Journal of Nanoscience and Technology **2**(3),144 (2016).
- [11] N. Topnani,S. Kushwaha, TaimurAthar, International Journal of Green Nanotechnology: Materials Science & Engineering,**1**,M67 (2009).
- [12] B. Satish, K.V. Rao, Ch. Shilpa Chakra, T. Dayakar, International Journal of Engineering Research & Technology (IJERT), **5**(5), 761 (2016).
- [13] H. Klug, L. Alexander, X-ray diffraction procedures, vol. 125 (Wiley, New York, 1962).
- [14] J. Tauc, Amorphous and Liquid Semiconductors (Plenum Press, New York, 1974), p. 171.